REPORT DOCUMENTATION PAGE	*Form Approved* *OMB No. 0704-0188*

1. REPORT DATE *(DD-MM-YYYY)* 14-09-2005	**2. REPORT TYPE** Journal Article	**3. DATES COVERED** *(From - To)*
4. TITLE AND SUBTITLE **Model for Ammonia Solar Thermal Thruster (POSTPRINT)**		**5a. CONTRACT NUMBER**
		5b. GRANT NUMBER
		5c. PROGRAM ELEMENT NUMBER
6. AUTHOR(S) Gianpiero Colonna, Giulia Capitta & Mario Capitelli (Università di Bari); Ingrid J. Wysong (AFRL/PRSA)		**5d. PROJECT NUMBER** 23080532
		5e. TASK NUMBER
		5f. WORK UNIT NUMBER
7. PERFORMING ORGANIZATION NAME(S) AND ADDRESS(ES) Air Force Research Laboratory (AFMC) AFRL/PRSA 10 E. Saturn Blvd. Edwards AFB CA 93524-7401		**8. PERFORMING ORGANIZATION REPORT NUMBER** AFRL-PR-ED-JA-2005-343
9. SPONSORING / MONITORING AGENCY NAME(S) AND ADDRESS(ES) Air Force Research Laboratory (AFMC) AFRL/PRS 5 Pollux Drive Edwards AFB CA 93524-7048		**10. SPONSOR/MONITOR'S ACRONYM(S)**
		11. SPONSOR/MONITOR'S NUMBER(S) AFRL-PR-ED-JA-2005-343

12. DISTRIBUTION / AVAILABILITY STATEMENT

Approved for public release; distribution unlimited (AFRL-ERS-PAS-2005-235)

13. SUPPLEMENTARY NOTES

©2005 by G. Colonna. Published by the American Institute of Aeronautics and Astronautics, Inc., with permission. Published in Journal of Thermophysics and Heat Transfer, AIAA 2005-4943.

14. ABSTRACT

This work is an attempt to investigate the nozzle expansion characteristics of a solar thruster that uses ammonia as propellant. For this purpose we have developed a state to state kinetic model to study the dissociation of ammonia in a supersonic nozzle expansion. The properties of the thruster depend on the ammonia dissociation degree in the reservoir, which can be very far from equilibrium due to the very slow dissociation kinetics at the thruster working conditions (<2000 K). We have extended the calculation for higher temperatures (>2500 K) where ammonia dissociation is higher. Due to the presence of some hydrogen atoms, non-Boltzmann distributions have been observed.

15. SUBJECT TERMS

16. SECURITY CLASSIFICATION OF:			**17. LIMITATION OF ABSTRACT**	**18. NUMBER OF PAGES**	**19a. NAME OF RESPONSIBLE PERSON** Dr. Ingrid J. Wysong
a. REPORT **Unclassified**	**b. ABSTRACT** **Unclassified**	**c. THIS PAGE** **Unclassified**	SAR	12	**19b. TELEPHONE NUMBER** *(include area code)* N/A

38th AIAA Thermophysics Conference
6 - 9 June 2005, Toronto, Ontario Canada

AIAA 2005-4943

A MODEL FOR AMMONIA SOLAR THERMAL THRUSTER

Gianpiero Colonna[1], Giulia Capitta[2] and Mario Capitelli,[3]
Dipartimento di Chimica, Università di Bari and CNR-IMIP, Bari, Italy, 70126

Ingrid J. Wysong[4]
Air Force Research Laboratory, PRSA, Edwards AFB, CA, 93524-7660, USA

and

Fred G. Kennedy, Major, United States Air Force[5]
Defense Advanced Research Projects Agency, Arlington, VA 22203

This paper is an attempt to investigate the nozzle expansion characteristics of a solar thruster that uses ammonia as propellant. For this purpose we have developed a state to state kinetic model to study the dissociation of ammonia in supersonic nozzle expansion. The properties of the thruster depend on the ammonia dissociation degree in the reservoir, which can be very far from equilibrium due to the very slow dissociation kinetics at the thruster working conditions (<2000 K). We have extended the calculation for higher temperatures (>2500 K) where ammonia dissociation is higher. Due to the presence of some hydrogen atoms, non-Boltzmann distributions have been observed.

Nomenclature

A = nozzle section
h = Plank constant
C_p = constant pressure heat capacity
C_v = constant volume heat capacity
c = speed of light
E_a = reaction activation energy
e = electron charge
K_d = rate coefficient of the direct reaction
K_{eq} = equilibrium constant
K_r = rate coefficient of the reverse reaction
P_0 = reservoir pressure
R = universal gas constant
T_0 = reservoir temperature
T_v = vibrational temperature
v = vibrational quantum number
α = C_v/R
α_D = ammonia dissociation degree
ε_v = vibrational level energy
γ = C_p/C_v

---

[1] Ph. D., Senior Researcher, e-mail: gianpiero.colonna@ba.imip.cnr.it, AIAA Member.
[2] Student, e-mail: jucapi@libero.it .
[3] Professor, e-mail: mario.capitelli@ba.imip.cnr.it , AIAA Member.
[4] Ph.D., Chief, Aerophysics Branch, ingrid.wysong@edwards.af.mil , AIAA Associate Fellow.
[5] Ph.D., Program Manager, Defense Advanced Research Projects Agency, fkennedy@darpa.mil, AIAA Senior Member

ω_e = first order spectroscopic constant to calculate vibrational level energies
$\omega_e x_e$ = second order spectroscopic constant to calculate vibrational level energies
$\omega_e y_e$ = third order spectroscopic constant to calculate vibrational level energies
$\omega_e z_e$ = fourth order spectroscopic constant to calculate vibrational level energies

I. Introduction

Recently, solar thermal propulsion (STP) engines have been investigated as a promising technology to enhance the capabilities of micosatellites maneuverability and enable new mission. Solar thermal propulsion takes advantage of concentrated sunlight—typically at concentration ratios of up to 10000:1—in order to raise a heat exchanger to temperatures of several thousands degrees K. At the Surrey Space Centre[1,2] (SCC), a small scale STP engine has been designed to use ammonia as propellant. The main advantage of ammonia as propellant is that it is a storable liquid with low molar mass and easy handling characteristics (and does not exhibit the serious toxicity and flammability risks posed by hydrazine).

To achieve improved performance, the ammonia gas is rapidly heated to 2000-2500 K, which should result in dissociation to N_2 and H_2 molecules, doubling the particle density and decreasing the average molecular weight of the mixture. This improves rocket performance by raising specific impulse (I_{sp}), which varies as the inverse square root of molecular weight. The problem is that the dissociation kinetics at temperatures of interest in the engine are very slow and therefore the complete dissociation of ammonia molecules may not occur.

In this paper we have developed a kinetic model for ammonia mixtures applied to the nozzle investigated at SSC[1,2]. It is worth noting that we have introduced state-to-state kinetics to verify the presence of non-equilibrium vibrational distributions during the nozzle expansion. We have also investigated the behaviors of the engine for higher reservoir temperatures (3000K-5000K) where the dissociation of ammonia is complete.

II. Model Description

A. Nozzle Geometry

The nozzle used in the thruster has a conic geometry of the following dimensions (in mm):

throat radius	0.35
exit radius	2.0
exit-throat distance	6.2
inlet radius	1.0
inlet-throat distance	1.2

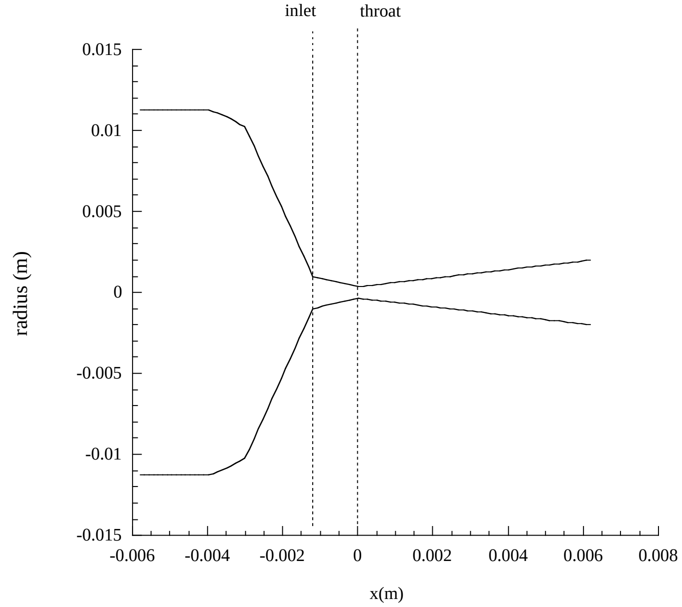

Figure 1. Nozzle profile.

These data have been provided by SSC researchers. The converging nozzle is quite short so we choose to include part of the reservoir in the calculation through a connecting cone of the following dimensions (in mm)

reservoir radius	11.25
connecting cone length	2.0

The nozzle is presented on fig 1.

The fluid dynamic model of the nozzle flow is based on the almost one-dimensional Euler equations for a variable section duct. The Euler equations are solved, for the stationary state, together with the perfect gas equation of state and the mass continuity for each species including the reaction contributions. The numerical scheme adopted is described in[3].

B. Chemical Model

To build the chemical kinetic models, we need to select both the species that must be taken into account and their mutual reactions. In the initial demonstration laboratory experiments, the pressure ranges from 1 to 4 atm and the temperature is less than 1500 K. For operational versions, the temperature could reach the value of 2500 K. The pressure values are measured directly, but the gas temperature is estimated from some measurements performed outside the reservoir. This results in a large uncertainty on the actual conditions operating inside the reservoir. For these temperatures the ammonia decomposition kinetics are quite slow. Surface dissociation, neglected in this approach, should, probably, be inserted in the model.

1. Species

We assume that the ammonia mixture consists of atoms and molecules formed in the NH_3 decomposition. We ignore all the ions because the temperatures involved are quite low. We introduce the vibrational excitation only for N_2 and H_2 molecules, which have stable vibrational excited levels. For all the other molecules, we diregard the internal levels as their number is so high that the computational load becomes unaffordable. A multitemperature model could be a valid approach assuring an acceptable computational cost nevertheless, in this work, we consider these internal states in equilibrium with the translational degree of freedom or as following a frozen kinetics. According to the internal state model selected we assign the C_p and γ ($\gamma = C_p/C_v$) coefficients to each molecule. For each vibrational mode or rotational axis, in equilibrium with the translational degree of freedom, we add the quantity αR into the expressions of C_p and C_v, where R represents the universal gas constant and the α parameter is set to 1 for a vibrational mode and to ½ for a rotational axis. This approximation is valid for the rigid rotor and for the infinite harmonic oscillator, since in general the C_p coefficient depends on the temperature. For atomic species no internal degree of freedom is considered. The contribution of translational degrees to the molar specific heat is 1.5R. Table 1 reports the species accounted and their relative properties.

Tab. 1: species inserted and their physical properties. Rot is the number of independent rotational axis, Vib the number of vibrational modes and E_f the enegy of formation.

Species	Mass (AMU)	Rot	Vib	E_f (eV)
NH_3	17	3	6	-0.403242
N_2H_3	31	3	9	4.30994
NH_2	16	3	3	2.00285
NH	15	2	1	3.90225
N_2	28	2	1	0.00000
H_2	2	2	1	0.00000
N	14	0	0	4.87950
H	1	0	0	2.23910

For H_2 and N_2 we estimate the energy of each vibrational level (ε_v) through the semi-empirical formula, function of the vibrational quantum number and of some spectroscopic constants expressed in cm^{-1}:

$$\varepsilon_v = \frac{hc}{e}\left[\omega_e\left(v+\frac{1}{2}\right) - \omega_e x_e\left(v+\frac{1}{2}\right)^2 + \omega_e y_e\left(v+\frac{1}{2}\right)^3 + \omega_e z_e\left(v+\frac{1}{2}\right)^4\right] \tag{1}$$

The H_2 spectroscopic constants have been obtained through the fits of the vibrational level energies extracted from the BKMP potential energy surface[4] while for N_2 we used data from ref. 5. Table 2 summarizes those values for the two species.

Table 2: Spectroscopic constants (in cm^{-1}) used in the calculation of the vibrational level energies.

Parameter	N_2	H_2
ω_e	2358.57	4464.7
$\omega_e x_e$	14.324	146.93
$\omega_e y_e$	-0.00226	4.7108
$\omega_e z_e$	0.0	-0.22712
E_{diss}	9.7639	4.4772
V_{max}	48	15

2. Processes

We implement in our model macroscopic kinetics for NH_3 depletion based on the following processes:

$$NH_3+X \leftrightarrow NH_2+H+X \quad (p1)$$
$$NH_3 + X \leftrightarrow NH + H_2 + X \quad (p2)$$
$$NH_3 + H \leftrightarrow NH_2 + H_2 \quad (p3)$$
$$NH + H + X \leftrightarrow NH_2 + X \quad (p4)$$
$$H_2 + N + X \leftrightarrow NH_2 + X \quad (p5)$$
$$NH_2 + H \leftrightarrow NH + H_2 \quad (p6)$$
$$NH_2 + NH_2 \leftrightarrow NH_3 + NH \quad (p7)$$
$$N + H + X \leftrightarrow NH + X \quad (p8)$$
$$NH + H \leftrightarrow H_2 + N \quad (p9)$$
$$NH + N \leftrightarrow N_2 + H \quad (p10)$$
$$NH + NH \leftrightarrow H_2 + N_2 \quad (p11)$$
$$2H + N_2 \leftrightarrow H_2 + N_2 \quad (p12)$$
$$2H + H_2 \leftrightarrow H_2 + H_2 \quad (p13)$$
$$2N + N_2 \leftrightarrow N_2 + N_2 \quad (p14)$$
$$2N + N \leftrightarrow N_2 + N \quad (p15)$$
$$NH_3 + NH_2 \rightarrow N_2H_3 + H_2 \quad (p16)$$
$$N_2H_3 + X \rightarrow NH_2 + NH + X \quad (p17)$$
$$N_2H_3 + H \rightarrow 2NH_2 \quad (p18)$$
$$N_2H_3 + H \rightarrow NH_3 + NH \quad (p19)$$

where X is a generic component. The rate coefficients for all these processes are expressed in the Arrhenius form:

$$K = K_0 T^{\delta} e^{-E_a/T} \quad (2)$$

For the direct reaction, the parameters K_0, δ and E_a are reported in Tab. 3. The rate coefficients of these processes have been taken from ref. 5-10. In this model, we neglect more complex molecules, such as N_2H_4, that do not seem to be significant.

Rates for the reverse processes have been obtained through the detailed balance principle

$$K_r = \frac{K_d}{K_{eq}} \quad (3)$$

where K_{eq} is the equilibrium constant. Equilibrium constants have been calculated, from partition functions, following the classical statistical thermodynamic theory[11]. Subsequently they have been fitted by the equation

$$\ln\left(K_{eq}\right) = K_{\infty} + K_p\left(\frac{1000}{T}\right)^{q_p} + K_e e^{-\frac{T}{q_e}} \quad (4)$$

We consider only the equilibrium constants for the generation of a new species from standard ones like N_2 and H_2 in nitrogen-hydrogen compounds formation. Therefore all the formation reactions can be synthesized as

$$\frac{n}{2}N_2 + \frac{m}{2}H_2 \leftrightarrow N_nH_m \quad (5)$$

The parameter values utilized to calculate K_{eq}, for the species listed in table 1 are reported in tab. 4.

Table 3: Arrhenius coefficients for the reactions inserted in the model. K_0 has the dimension of $cm^{3(n-1)}/s$, where n is the number of particles involved in the reaction, E_a is expressed in K and δ is a dimensionless parameter (eq. 2).

process	K_0	δ	E_a	Ref.
p1	1.53e-8	0	42400	6
p2	1.00e-9	0	47000	4
p3	3.20e-13	0.67	1720	5
p4	1.00e-32	0	0	7
p5	1.00e-34	0	0	7
p6	2.30e-13	0.67	2160	5
p7	6.64e-12	0	2800	6
p8	1.00e-33	0	0	7
p9	1.70e-12	0.68	957	5
p10	1.77e-11	0	0	5
p11	6.60e-13	0.55	957	5
p12	1.34e-31	-0.60	0	5
p13	2.68e-31	-0.60	0	5
p14	7.44e-32	-0.50	0	5
p15	3.31e-27	-1.50	0	5
p16	1.33e-12	0.5	10850	4
p17	1.70e-8	0.	21000	4
p18	2.60e-12	0	0	4
p19	1.70e-13	0	0	4

Table 4: Coefficients used to calculate the formation equilibrium constants when the pressures are expressed in Pa.

Species	K_∞	K_p	q_p	K_e	q_e
NH_3	51.8293	-13.1631	0.960208	-7.97367	628.095
NH_2	19.6666	63.4542	1.01863	13.5452	311.287
NH	-5.14978	85.2911	0.998065	-2.21874	423.673
N	28.3772	-114.298	0.997620	-2.14877	4371.66
H	26.1506	-52.7759	0.996362	-2.71911	2157.34

From these formation equilibrium constants we can calculate the equilibrium constants relative to all the reactions involving the species in the table.

The kinetic model has been improved including state-to-state kinetics for the diatomic species N_2 and H_2, substituting processes P12-P15 with the state-selective dissociation and adding vibrational relaxation processes[12-14]

$$N_2(v) + N_2(w) \leftrightarrow N_2(v-1) + N_2(w+1) \tag{p20}$$

$$N_2(v) + N_2(w) \leftrightarrow N_2(v-1) + N_2(w) \tag{p21}$$

$$N_2(v) + N \leftrightarrow N_2(v-\Delta v) + N \tag{p22}$$

$$N_2(v) + N_2(w) \leftrightarrow N_2(v-1) + 2N \tag{p23}$$

$$N_2(v) + N_2(w) \leftrightarrow 2N + N_2(w) \tag{p24}$$

$$N_2(v) + N \leftrightarrow 2N + N \tag{p25}$$

$$H_2(v) + H_2(w) \leftrightarrow H_2(v-1) + H_2(w+1) \tag{p26}$$

$$H_2(v) + H_2(w) \leftrightarrow H_2(v-1) + H_2(w) \tag{p27}$$

$$H_2(v) + H \leftrightarrow H_2(v-\Delta v) + H \tag{p28}$$

$$H_2(v) + H_2(w) \leftrightarrow H_2(v-1) + 2H \tag{p29}$$

$$H_2(v) + H_2(w) \leftrightarrow 2H + H_2(w) \tag{p30}$$

$$H_2(v) + H \leftrightarrow 2H + H \tag{p31}$$

All the other processes involve only the ground state of such molecules. We have also included vibrational relaxation of nitrogen molecues due to hydrogen[5,8]:

$$N_2(v) + H_2(w) \leftrightarrow N_2(v-1) + H_2(w) \tag{p32}$$

$$N_2(v) + H \leftrightarrow N_2(v-\Delta v) + H \tag{p33}$$

$$N_2(v) + H_2(w) \leftrightarrow N_2(v-1) + H_2(w+1) \tag{p34}$$

III. Results

C. Low reservoir temperature (T<2500 K)

In this paragraph we want to investigate the kinetic behavior of the ammonia mixture in cases close to the working conditions of the solar thruster studied at the Surrey Space Centre[1,2]. The pressure range is between 1 and 4 Bar and the temperature is < 1500 K. The heater temperature is not well known because it has been mesured[1,2] outside the chamber. We have extended our calculations to temperature values below 2500 K, which may be obtained in orbital conditions.

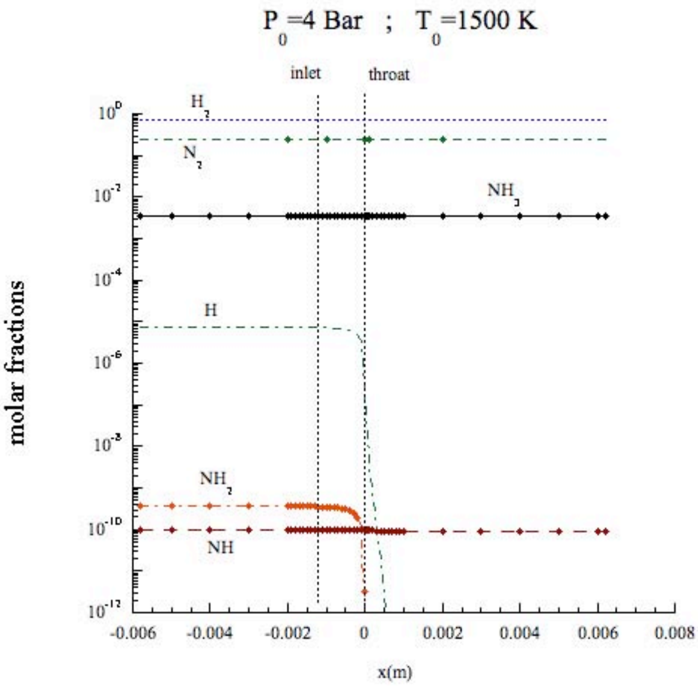

Figure 2: Molar fractions of mixture species along the nozzle. We assume as reservoir conditions P_0=4 Bar and T_0=1500 K and start from an equilibrium inlet composition.

We investigate four different pressure values in the range 1-4 Bar. In figure 2 we report the concentration profiles along the nozzle obtained for reservoir conditions of P=4 Bar and T=1500 K, and introducing the vibrational kinetics of N_2 and H_2.

It is interesting to observe that the flow is practically frozen along the whole nozzle except for some minor species such as H and NH_2 that completely disappear at the nozzle exit. The atomic nitrogen molar fraction is lower than 10^{-10}.

Figures 3 and 4 describe the vibrational distribution of hydrogen and nitrogen for the conditions of figure 2. We can observe that the nitrogen distributions are frozen. On the contrary, while H_2 distributions, for $v \leq 3$, are almost frozen, their tails are strongly depleted, resulting in non-Boltzmann distributions. The different behavior of the two species is due to the different percentage of nitrogen and hydrogen atoms; hydrogen atom concentration is high enough so that the VT collisions involving atoms are frequent enough to cool the distribution tails. We observe that the Mach number is practically independent of the initial temperature and pressure, obtaining at the nozzle exit a value close to Mach 5.4. We report the pressure along the nozzle in figure 5. It is quite interesting to note that the exit pressure is proportional to the inlet pressure. These two results occur as the chemistry weakly affects the macroscopic quantities during the expansion.

Table 5 reports the mass flow rate and the thrust for different inlet pressures at T_0=1500 K or T_0=2500 K. The agreement with the experimental results reported in table 6 is satisfactory, as the nozzle reservoir conditions (mainly the temperature) are not well known experimentally.

In this temperature range the kinetics of ammonia presents large uncertainties[5-8], even though it has been widely studied. The main problem is that the slow kinetics prevents us from estimating the kinetic constant precisely. Experimental works[1,2] on ammonia thrusters assume a complete decomposition of ammonia in the reservoir, but the kinetic scheme proposed does not permit to reach the equilibrium condition in an acceptable time for T<2000 K. Under these conditions the most important problem is that it is possible that in the inlet conditions there is not equilibrium as usually happens in nozzle reservoirs. Because of this we also try as initial condition a pure ammonia gas.

Dissociation inside the reservoir and the nozzle is very poor, so that again in this case the flow is frozen. As a consequence, the flow properties depend only on the C_p/C_v ratio and on the mean molar mass, so the exit properties are completely different form the equilibrium case. As an example in figure 6 we compare the Mach numbers computed starting from an equilibrium composition (Eq.) and from pure ammonia (NoEq.). It is not possible to really know what composition prevails inside the reservoir for T<2000K, moreover some impurites or wall catalytic effects can accelerate the kinetics, bringing the system to equilibrium faster than predicted by our kinetic model.

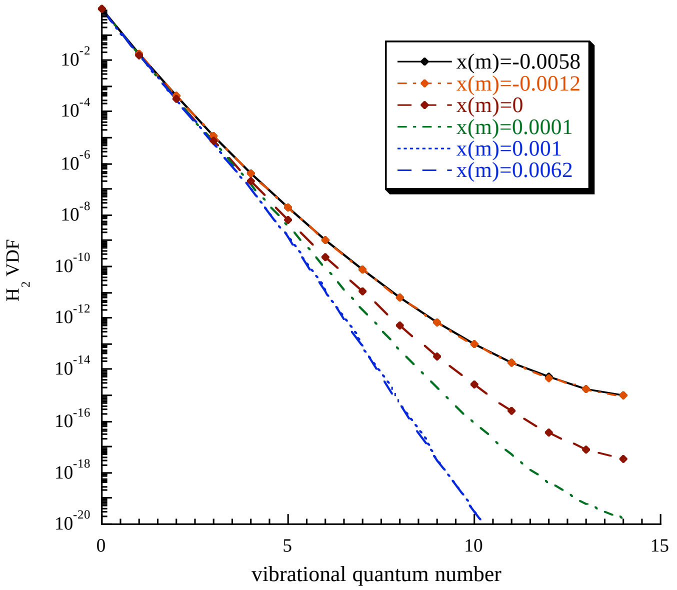

Fig. 3: Hydrogen vibrational distributions at different nozzle positions in the same conditions as in fig. 2.

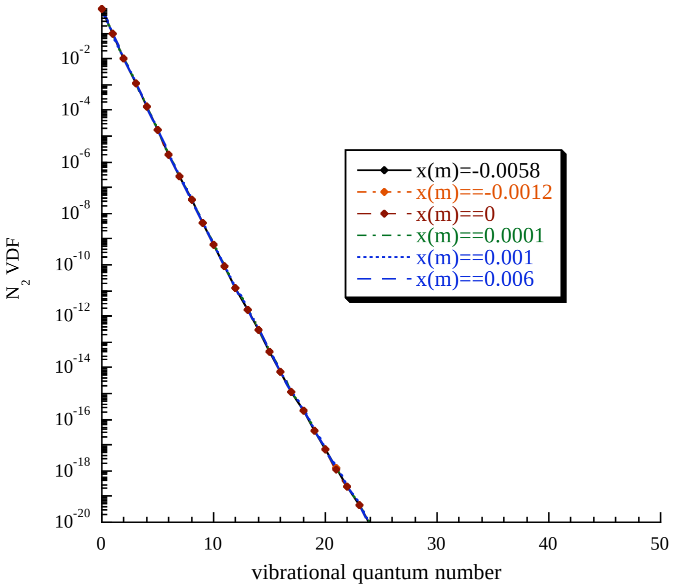

Figure 4: Nitrogen vibrational distributions at different nozzle positions in the same conditions as in fig. 2.

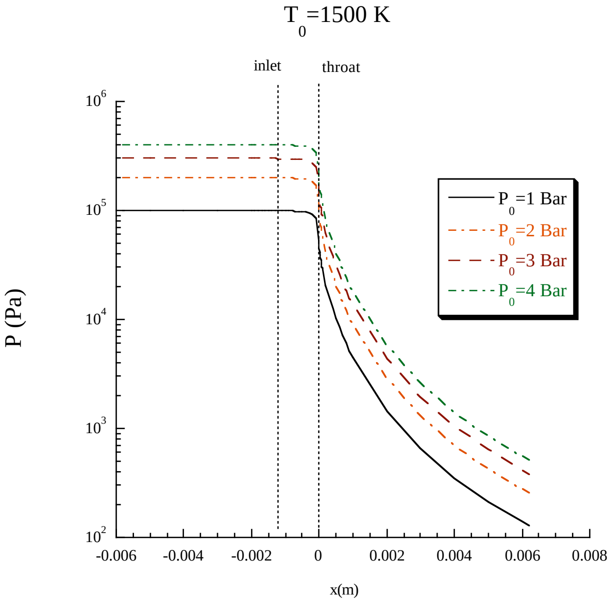

Fig. 5: Pressure profile along the nozzle as a function of the inlet pressure for T_0=1500 K and starting from an inlet equilibrium composition.

Table 5: Computed mass flow rate and thrust of the nozzle as a function of the inlet pressure. The inlet temperature is T_0=1500 K except when marked with the "*" symbol assigned to T_0=2500 K. At the inlet we suppose an equilibrium composition.

P_0(Bar)	mass flow rate (g/s)	thrust (mN)
1	2.1708e-2	64.337
2	4.3404e-2	128.68
3	6.5077e-2	192.97
4	8.6784e-2	257.38
4*	6.5954e-2	256.74

* T=2500 K

Table. 6: Mass flow rate and thrust of the nozzle determined experimentally in different test cases.

mass flow rate (g/s)	thrust (mN)
.140	219
.147	223
.117	183
.121	190

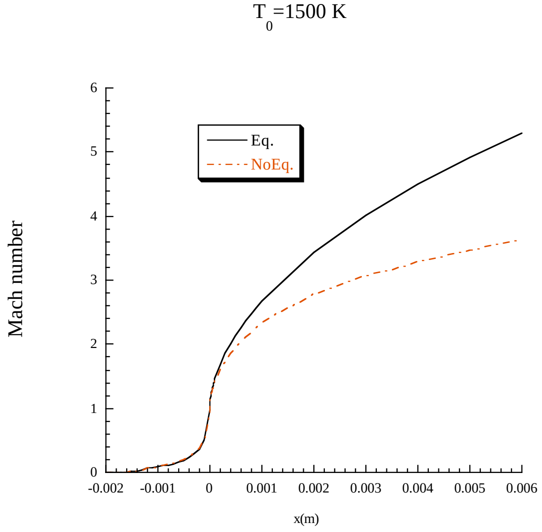

Figure 6: Mach number profile compared for inlet equilibrium (Eq) and pure ammonia (noEq) case (pressure and temperature conditions as in fig 2).

Table 7: Computed mass flow rate and thrust as a function of the inlet dissociation degree (α_D) of the ammonia. Inlet pressure and temperature are P_0=4 Bar and T_0=1500 K.

α_D	mass flow rate (g/s)	thrust (mN)	I_{sp}
0.0	1.1189e-1	284.13	259
0.2	1.0437e-1	280.35	274
0.4	9.7946e-2	275.67	287
0.8	8.9483e-2	264.37	296
1.0	8.5450e-2	253.33	302

We try the same comparison at T_0=2500 K. In this case, the mixture reaches the equilibrium composition in the reservoir. Nevertheless, the Mach number profiles in the equilibrium and non equilibrium case are again different (see fig. 7). This is the demonstration that the history of the gas in the reservoir is important.

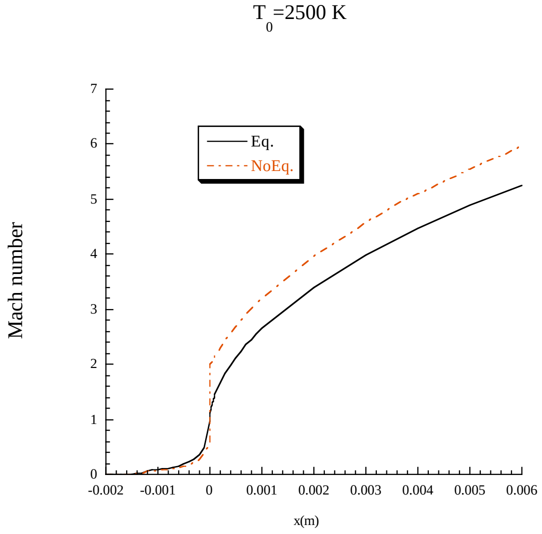

Figure 7: Same as in fig 6 with reservoir temperature T_0=2500 K and pressure P_0=4 Bar.

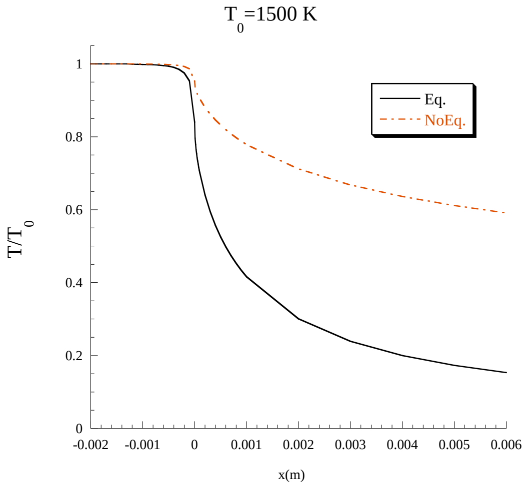

Figure 8: Reduced temperature profile compared for inlet equilibrium (Eq) or pure ammonia (noEq) case (pressure and temperature conditions as in fig 2).

Effects of initial conditions propagate also on the temperature profiles. In figure 8 we show the normalized temperature profile calculated starting from an equilibrium condition (Eq.) and from an undissociated ammonia (NoEq.) for a reservoir temperature of 1500 K and a pressure of 4 Bar. We observe that the exit temperature is much higher in the case of the equilibrium conditions. This behaviour could be due to the lower mean molar mass associated with the mixture in equilibrium composition inside the reservoir.

Different behaviours occur when the reservoir temperature reaches 2500 K (see fig. 9). In fact, at this temperature, the reactions in the inlet are faster than in the flow, therefore one can observe an increase of the temperature due to the mixture dissociation. Even if the ammonia energy is lower than that of nitrogen and hydrogen molecules, the compression due to the double particle number density produces an increase of the temperature. At the nozzle exit, the differences are lower than in the case of an inlet temperature of 1500 K.

We find similar behaviours for the relaxation of the vibrational temperature, calculated as the temperature of the first excited level (figure 10). Starting from non equilibrium conditions we can observe an increase of the vibrational temperatures following the gas temperature. At the nozzle exit the vibrational temperature freezes at a temperature higher than 2300 K just after the throat. N_2 vibrational temperature is practically frozen.

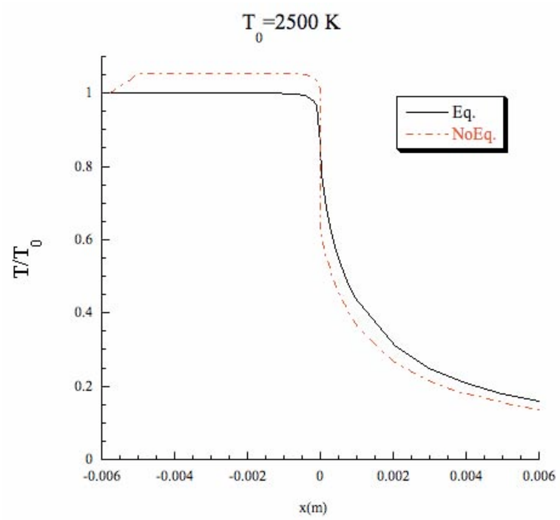

Fig. 9: Reduced temperature profile compared for inlet equilibrium (Eq) or pure ammonia (noEq) case, for a reservoir temperature T_0 = 2500K (pressure and temperature conditions as in fig 2).

As a consequence of the previous results, we can state that there are some uncertainties about the inlet composition. To demonstrate the sensitivity we have reported in table 7 the calculated mass flow rate and thrust for different dissociation degrees "α_D"of ammonia for the process NH_3 = 1.5 H_2 + 0.5 N_2 defined as

$$\alpha_D = 1 - \frac{[NH_3]}{[NH_3] + .5[N_2]}$$

that ranges from 0 (pure ammonia) to 1 (N_2 and H_2 mixture). We note that both quantities decrease when the dissociation degree increases, but the thrust changes more slowly than the mass flow rate, so the specific impulse will be higher for the dissociated case.

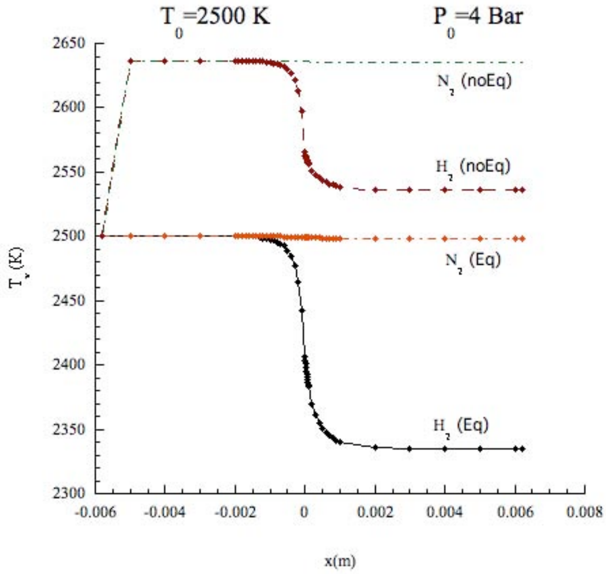

Figure 10: Vibrational temperature (T_v) profile of N_2 and H_2 in the same conditions as in figure 9.

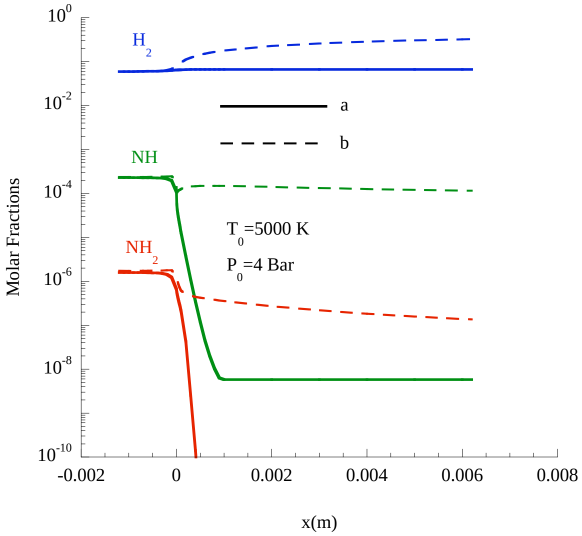

Figure 11: Molar fraction profiles calculated with different kinetic models.

D. High reservoir temperature (T>2500 K)

In the previous paragraph we have studied the behavior of the ammonia solar thruster in the working conditions of the thruster investigated experimentally in refs. 1,2. In this paragraph we want to understand the behaviors of the thruster for higher temperature ranges (3000 K $\leq T_0 \leq$5 000 K). For temperature T_0>2500 the ammonia dissociation is very fast.

Moreover in the considered temperature range the molar fraction of atomic hydrogen is not negligible. In this conditions, due to the recombination of hydrogen atoms and to atom-molecule VT collisions, non equilibrium vibrational distributions can be observed and non-Arrhenius chemical rates are obtained[12], inducing anomalous behaviors in the kinetics.

Here we want to focus on the differences between the results obtained with two different models:

a - macroscopic kinetics
b - state to state kinetics.

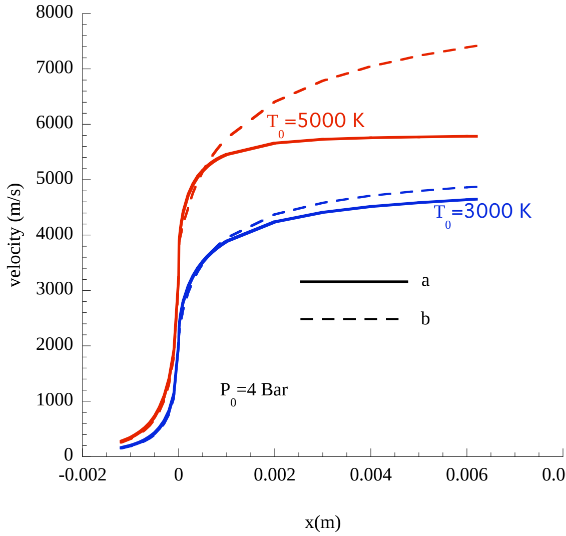

Figure 12: Velocity profiles calculated with different kinetic models.

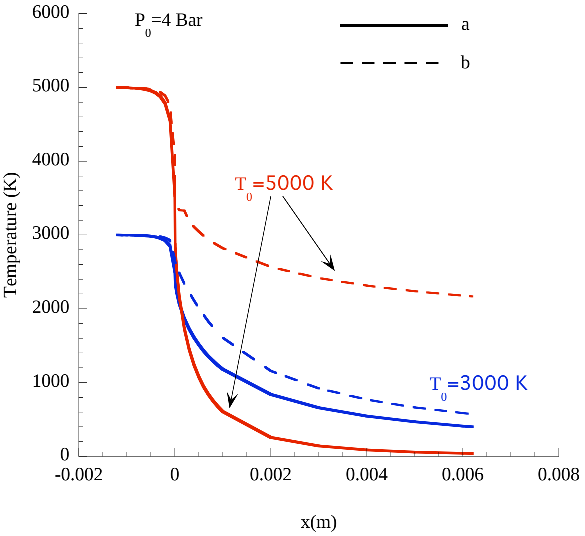

Figure 13: Temperature profiles calculated with different kinetic models.

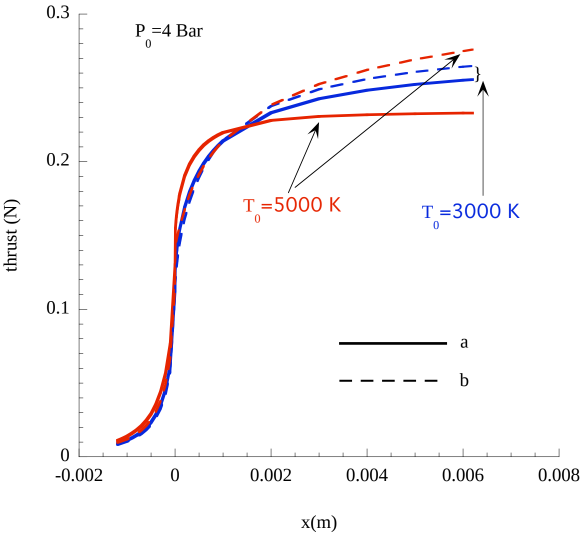

Figure 14: Thrust profiles calculated with different kinetic models.

In fig. 11 we have compared the molar fractions of some species calculated with the two models. It is possible to observe that H_2 molar fraction increases when the state to state model is considered, while the macroscopic model predicts a frozen concentration. On the contrary, NH_2 and NH molar fractions show smaller variations when the state to state approach is used.

This behavior affects the macroscopic quantities such as the gas speed, the temperature and the thrust. In fig. 12 we have compared the axial speed profile in the two kinetic models at two different reservoir temperatures. There are appreciable differences at the nozzle exit especially for reservoir temperature T_0=5000 K. This effects is the consequence of the stronger recombination of hydrogen atoms in the H_2 molecules as can be observed in figure 11. Similar behaviors can be observed in the gas temperature profile (fig. 13) and in the thrust (fig. 14). An important result is that the calculated thrust (and therefore the performances) is higher when the state to state vibrational kinetic model is included in the calculation.

IV. Conclusion

In this paper we have investigated the chemical kinetic aspects of an ammonia mixture for application to solar thermal thrusters. We have obtained results that contradict the common assumption of considering inlet conditions in equilibrium. If the kinetics of the mixture is very slow, as in the case of ammonia, the gas composition can be far from equilibrium. At low reservoir temperature (T_0<2500 K), that is the working condition for the thruster in the laboratory, the kinetics of internal states is negligible, and the macroscopic and state to state models gives the some results, mainly because the flow is almost frozen. On the other end, at higher reservoir temperature (T_0≥3000 K), when the hydrogen dissociation is important, the vibrational kinetics becomes very important. In these conditions the macroscopic and the state to state model predict different results, mainly due to the different atomic recombination.

We must emphasize that this study is preliminary. Some properties of the mixtures have been neglected, such as the vibrational energy of the NH_x molecules and the formation of NH molecules by vibrationally excited N_2 and H_2. The model can be improved including a multitemperature approach to account for the vibration of polyatomic molecules and by adding new state to state reactions between N_2 and H_2.

Acknowledgments

This work has been supported by U.S. Air Force European Office of Aerospace Research and Development.

References

[1] Kennedy, F., Palmer, P. and Paul, M., “Microscale Solar Thermal Engine Ground Test Campaign at the Surrey Space Centre” *AIAA-2004-4137*.

[2] Kennedy, F. and Palmer, P., “A Comparison of Simulation and Test Campaign Results for a Microscale Solar Thermal Engine” 54th international Astronautical Congress, Sept. 29th – Oct. 3rd 2003, Bremen, Germany.

[3] Colonna, G., Tuttafesta, M. and Giordano, D., "Numerical Methods to Solve Euler Equations in One-dimensional steady Nozzle Flow" *Computer Physics Communications*, Vol. 138, 2001, pp. 213-221.

[4] Boothroyd, A. I., Keogh, W. J., Martin, P. G. and Peterson, M. R., "A Refined H_3 Potential Energy Surface ", *Journal of Chemical Physics*, Vol. 104, 1996, pp. 7139-7169.

[5] Capitelli, M., Ferreira, C.M. and Gordiets, B.F., *Plasma Kinetics in Atmospheric Gases*, Ed. Springer, Berlin, Germany, 2000.

[6] Starikovskaia, S.M., Starikovskii, A. Yu. and Zatsepin, D.V., “Hydrogen oxidation in a stoichiometric hydrogen-air mixture in the fast ionization wave”, *Combustion Theory and Modeling*, Vol. 5, 2001, pp. 97-129.

[7] Yasui, K., “Chemical Reactions in Sonoluminescing Bubble”, *Journal of the Physical Society of Japan*, Vol. 66, 1997, pp. 2911-2920.

[8] Gordiets, B., Ferreira, C.M., Pinheiro, M.J., Ricard, A., “Self consistent kinetic model of low pressure N_2-H_2 flowing discharges: I. Volume processes”, *Plasma Sources Science and Technology*, Vol. 7, 1998, pp. 363-378.

[9] Yumura, M., Asaba, T., Matsumoto, Y. H. Matsui, Y., “Thermal decomposition of Ammonia”, *Journal of Computational Chemistry*, Vol. 1, 1980, pp. 439-450.

[10] Davidson, D. F., Kohse-Höingaus, K., Chang, A. Y. and Hanson, R. K., “A Pyrolisis Mechanism for Ammonia”, *International Journal of Chemical Kinetics*, Vol. 22, 1990, pp. 513-535.

[11] Landau, L.D., *Statistical Physic*, Ed. Elsevier Sciences, Amsterdam, Netherlands, 1979.

[12] Colonna, G., Tuttafesta, M., Capitelli, M. and Giordano, D, "Non-Arrhenius NO Formation Rates in One-Dimensional Nozzle Airflow", *Journal of Thermophysics and Heat Transfer*, Vol. 13, No 3, 1999, pp. 372-375.

[13] Capitelli, M., Colonna, G. and Esposito, F., “On The Coupling Of Vibrational Relaxation With The Dissociation-Recombination Kinetics: From Dynamics To Aerospace Applications”, *Journal of Physical Chemistry A*, Vol 108, 2004, pp. 8930-8934.

[14] Colonna, G., Esposito, F. and Capitelli, M., “H_2 state to state kinetics in nozzle expansion”, July 10-16, 2004, Porto Giardino, Monopoli (Bari), Italy (in press).